Biochimica et Biophysica Acta 1853 (2015) 724–732

Contents lists available at ScienceDirect

Biochimica et Biophysica Acta

journal homepage: www.elsevier.com/locate/bbamcr

A novel mitochondrial carrier protein Mme1 acts as a yeast mitochondrial magnesium exporter

Yixian Cui [a,*,1], Shanke Zhao [a,1], Juan Wang [a,2], Xudong Wang [a], Bingquan Gao [b], Qiangwang Fan [a], Fei Sun [b], Bing Zhou [a,**]

[a] State Key Laboratory of Biomembrane and Membrane Biotechnology, School of Life Sciences, Tsinghua University, Beijing 100084, China
[b] Institute of Biophysics, Chinese Academy of Sciences, Beijing 100101, China

ARTICLE INFO

Article history:
Received 31 July 2014
Received in revised form 28 November 2014
Accepted 22 December 2014
Available online 10 January 2015

Keywords:
Lpe10
mitochondrial Mg^{2+} exporter
Mme1
Mrs2
proteoliposome

ABSTRACT

The homeostasis of magnesium (Mg^{2+}), an abundant divalent cation indispensable for many biological processes including mitochondrial functions, is underexplored. Previously, two mitochondrial Mg^{2+} importers, Mrs2 and Lpe10, were characterized for mitochondrial Mg^{2+} uptake. We now show that mitochondrial Mg^{2+} homeostasis is accurately controlled through the combined effects of previously known importers and a novel exporter, Mme1 (mitochondrial magnesium exporter 1). Mme1 belongs to the mitochondrial carrier family and was isolated for its mutation that is able to suppress the *mrs2Δ* respiration defect. Deletion of *MME1* significantly increased steady-state mitochondrial Mg^{2+} concentration, while overexpression decreased it. Measurements of Mg^{2+} exit from proteoliposomes reconstituted with purified Mme1 provided definite evidence for Mme1 as an Mg^{2+} exporter. Our studies identified, for the first time, a mitochondrial Mg^{2+} exporter that works together with mitochondrial importers to ensure the precise control of mitochondrial Mg^{2+} homeostasis.

1. Introduction

Magnesium (Mg^{2+}) is a major intracellular divalent cation in living cells. As a critical co-factor for hundreds of enzymes, Mg^{2+} has been known to participate in over 300 metabolic reactions, including but not limited to energy production, ion metabolism, and cell cycle regulation [1]. Mg^{2+} also plays an important role in sustaining genomic stability and preventing carcinogenicity [2]. Therefore, it is quite apprehensible that alterations in Mg^{2+} metabolism would correlate to many important human diseases [3], including metabolic syndromes such as type 2 diabetes mellitus and hypertension [4]. In higher plants, Mg^{2+} also plays a critical role in regulating the chloroplast mRNA stability [5].

Saccharomyces cerevisiae has been proved to be an excellent model organism for the study of many fundamental biological processes, including the mechanism of Mg^{2+} transport. Up to now, three types of Mg^{2+} transporters have been identified in yeast—the Alr Mg^{2+} transport system in the cell plasma membrane, the Mnr2 Mg^{2+} transporter in the vacuolar membrane, and the Mrs2/Lpe10 Mg^{2+} transporter in the mitochondrial inner membrane.

The two Alr proteins (Alr1 and Alr2) are orthologues of the bacterial CorA transporter, sharing with the latter a highly conserved GMN motif [6]. Both Alr1 and Alr2 localize in the plasma membrane and function as Mg^{2+} uptakers [6,7].

In vacuoles, storage sites for Mg^{2+} within yeast cells, a Mg^{2+}/H^{+} exchange mechanism was discovered to drive Mg^{2+} entry into the organelles [8]. On the other hand, Mnr2 (manganese resistance 2)—a vacuolar membrane protein that functions as a putative Mg^{2+} transporter and shares similarities with Alr1 and Alr2—is responsible for Mg^{2+} efflux from vacuoles. Genetic evidence shows that this protein functions by releasing Mg^{2+} into the cytosol under Mg^{2+}-deficient conditions [9].

Besides vacuoles, mitochondria serve as another intracellular Mg^{2+} pool. Two mitochondrial Mg^{2+} transporters, Mrs2 and Lpe10, were reported to be responsible for the influx of Mg^{2+} into mitochondria [10–13]. *MRS2* (mitochondrial RNA splicing 2) was initially identified for its requirement in mitochondrial group II intron splicing and growth on non-fermentable media [10]. This is a result of its intramitochondrial Mg^{2+} deficiency affecting the ribozyme [11] because Mrs2 plays an essential role in mitochondrial Mg^{2+} influx [12]. The decrease in mitochondrial Mg^{2+} content of the *mrs2Δ* mutant can be

Abbreviations: FC12, Fos-choline-12; ICP-MS, inductively coupled plasma mass spectrometry; IPTG, isopropyl-β-D-thiogalactopyranoside; Mg^{2+}, magnesium; RT-PCR, reverse transcription polymerase chain reactions

* Corresponding author. Tel./fax: +86 10 62772253.
** Corresponding author. Tel.: +86 10 62795322; fax: +86 10 62772253.
E-mail addresses: cuiyx07@gmail.com (Y. Cui), zhoubing@mail.tsinghua.edu.cn (B. Zhou).
[1] These authors contributed equally to this work.
[2] Present address: Department of Cellular and Molecular Medicine, University of California at San Diego, La Jolla, CA 92093-0668, USA.

http://dx.doi.org/10.1016/j.bbamcr.2014.12.029
0167-4889/

rescued by the expression of bacterial Mg^{2+} transporter CorA fused to a mitochondrial N-terminal leader sequence of *MRS2* [13]. The functional complementation was also observed with the orthologue of Mrs2 in humans [14].

Yeast Lpe10 also localizes at the mitochondrial inner membrane and shares 32% of its sequence identity and a conserved GMN motif with Mrs2 [15]. Similarly, Lpe10 disruptant exhibited defects in both growth on glycerol-based media and RNA processing, together with a reduction in the mitochondrial Mg^{2+} content. Overexpression of *LPE10* leads to a sharp increase of Mg^{2+} in mitochondria, indicating its structural and functional similarities to Mrs2 [15]. A tight interaction between Lpe10 and Mrs2 and their hetero-oligomerization was discovered [16]. However, these two proteins cannot fully substitute for one another, indicating that their functions are not redundant. In fact, deletion of *LPE10* leads to a decrease in the mitochondrial membrane potential, which is not observed when *MRS2* is deleted [16].

To investigate whether other partners might be involved in the regulation of Mg^{2+} homeostasis in mitochondria, we arranged a genetic screening to look for the suppressors of the *mrs2Δ* mutant. Previously, we isolated a novel gene *YMR166C* as a candidate involved in mitochondrial Mg^{2+} homeostasis [17]. However, we were uncertain about how exactly YMR166C is involved in this process. We now show that YMR166C is a mitochondrial Mg^{2+} exporter. We renamed *YMR166C* to *MME1* (mitochondrial magnesium exporter 1). Mitochondrial Mg^{2+} homeostasis turns out to be a finely controlled process directed by the combinatory work of the importers and the exporter.

2. Materials and Methods

2.1. Strains, growth medium, and plasmids

Yeast transformation was carried out by the standard lithium acetate method [18]. Empty vectors were transformed in parallel to serve as negative controls. Single colonies of each transformed yeast strain were picked out and grown on synthetic selective media. Glucose (2%) was added into YPD or SD medium, while 2% glycerol was added into YPG or SG medium. The SD-Mg^{2+} media used in this study were prepared with a yeast nitrogen base without the addition of $MgSO_4$. The SD-Mg^{2+} media were carefully prepared with ultra-pure water, high-purity reagents (≥99.99%), and a clean container to avoid any Mg^{2+} contamination.

Expression plasmids used in yeast were pRS315, pGPD-413, and pTEF-425 obtained from ATCC [19]. For heterologous expression in *E. coli*, the plasmid used was a home-made pEXS-DH, generated on the backbone of pET-22b(+). The region between the T7 transcription start and T7 terminator was replaced by an N-terminal 8 × HIS tag sequence followed by a TEV cleavage site and a C-terminal 8 × HIS tag sequence. The linker sequence had been optimized for protein expression.

2.2. Measurement of metal content in isolated mitochondria

Isolation of yeast mitochondria was performed according to a previous protocol [20]. Protein level of each mitochondrial sample was determined by the BCA Protein Assay Kit (Thermo Scientific Pierce, Waltham, MA, USA). The content of each metal ion was determined by inductively coupled plasma mass spectrometry (ICP-MS) XII (Thermo Electron Corp., Waltham, MA, USA) by the Analysis Center of Tsinghua University.

2.3. Measurement of mitochondrial Mg^{2+} by spectrofluorometry

Mitochondria were isolated from cells of the wild-type and *mme1Δ* mutant and then transferred into a nominally Mg^{2+}-free solution for loading of the Mg^{2+}-sensitive fluorescent dye, mag-fura-2-AM (Molecular Probe). Loading was performed by incubating mitochondria (0.5 mg/ml) in SH buffer (0.6 M sorbitol, 20 mM HEPES ± KOH; pH = 7.4) with 5 μM mag-fura-2-AM for 35 min at 25 °C. Mitochondria were subsequently washed three times with SH buffer to remove excess fluorescent dye. A further incubation for 35 min was carried out to allow a complete hydrolysis of the fluorescent dyes, and the mitochondria were washed twice before measuring the fluorescence intensity. To analyze Mg^{2+}-dependent changes in mitochondria, external Mg^{2+} was elevated successively to a final concentration of 10 or 20 mM. Fluorescence intensities at 340 nm and 380 nm were recorded continuously [12]. Concentrations of intra-mitochondrial Mg^{2+} were calculated from the 340/380 nm ratio according to the formula of Grynkiewicz et al. with a dissociation constant of the mag-fura-2 ± Mg^{2+} complex of 1.52 in SH buffer and 1.89 in KCl buffer (150 mM KCl, 300 mM sucrose, 20 mM HEPES ± KOH; pH = 7.4) [21].

2.4. Protein purification

Mme1 protein was expressed in *E. coli* CD41 (DE3) cells cultured in 4 L LB media containing ampicillin. Isopropyl-β-D-thiogalactopyranoside (IPTG, 0.5 mM) was added into the cells at an OD_{600} of about 0.3 to induce protein expression at 16 °C for 16–20 h. The culture was then harvested and resuspended (0.1 g/ml) in buffer A (20 mM Tris, 150 mM NaCl, 2 mM phenylmethylsulfonylfluoride, 1 mg/ml DTT, 1 mg/ml RNAase; pH = 7.5) and broken by French pressure cell at 16,000 p.s.i three times. Unbroken cells and inclusion bodies were removed by centrifugation at 24,000 *g* for 40 min at 4 °C. Then, the supernatant was again centrifuged with 250,000 *g* for 1 h and 10 min. The pellet (membrane and membrane proteins) was resuspended and dissolved with buffer B (20 mM Tris, 150 mM NaCl, 2 mM phenylmethylsulfonylfluoride, 30 mM imidazole; pH = 7.5). FC12 was added to a final concentration of 0.15% (w/v), and the unsolubilized pellet was centrifuged at 200,000 *g* for 30 min at 4 °C. The supernatant containing the Mme1 protein was then purified by nickel-affinity chromatography. Briefly, the supernatant was loaded onto a 1 ml volume of pre-equilibrated Ni-NTA agarose column (Invitrogen) and washed with 30 column volumes of buffer B. The column-bound protein was eluted with 5 column volumes of buffer C (20 mM Tris, 150 mM NaCl, 2 mM phenylmethylsulfonylfluoride, 300 mM imidazole, 0.15% FC12; pH = 7.5). To further purify the protein and dissolve the protein in buffer suitable for the following proteoliposome experiments, the eluted protein was passed through a Sephadex 200 column with buffer D (20 mM HEPES, 100 mM KCl, 15 mM $MgCl_2$, 0.5 mM ATP-Mg, 0.15% FC12; pH = 7.0) [22].

2.5. Mg^{2+} transport assay of reconstituted proteoliposomes

Assays of Mg^{2+} transport activity of Mme1 in proteoliposomes were accomplished according to the published methods with some modifications [22,23]. Chloroform–methanol (3:1) was added to dissolve the yeast total lipids (Avanti Polar Lipids, Inc. Alabama, USA), and the lipids were subsequently dried in a rotary evaporator at 30 °C for another 30 min to remove the methanol and traces of chloroform. The dried lipids were suspended at room temperature to a final concentration of 10 mg/ml in buffer E (20 mM HEPES, 100 mM KCl, 15 mM $MgCl_2$, 0.5 mM ATP-Mg; pH = 7.0). The lipid suspension was then sonicated to generate a suspension of small unilamellar vesicles (SUVs). The SUV suspension was then flash-frozen in liquid N_2 and subsequently slowly thawed at room temperature for three cycles. Mg^{2+} was loaded into the liposomes using the above steps. The liposomes were then destabilized by the addition of 0.5% (w/v) Triton X-100 and incubated for 3 h at room temperature with agitation. Afterwards, purified Mme1 was added with a lipid/protein ratio of 40:1 (w/w), and the mixture containing 0.5% (w/v) Triton X-100 was incubated for 2 h at 4 °C with agitation. The detergents were removed by incubating the mixture for 1–2 h at 4 °C with agitation with additional Bio-Beads SM-2 (Bio-Rad) at a

bead (wet weight)/detergent ratio of 60:1 (w/w). Bio-Beads SM-2 were then removed from the solution, and a second aliquot of Bio-Beads SM-2 was added. The sample was incubated for 2–3 h at 4 °C with agitation. The proteoliposome solution was separated from the Bio-Beads SM-2 and then centrifuged at 210,000 *g* for 30 min at 4 °C. The pellets of liposome were resuspended in buffer F (20 mM HEPES, 100 mM NaCl; pH = 6.0). To ensure more complete Mg^{2+} transport by Mme1, the suspension of liposomes was incubated at 30 °C for 2 h. Finally, the liposomes were spun down and washed with corresponding reaction buffer F twice and the Mg^{2+} contents within the liposomes were determined by ICP-MS. The influx measurements were similar with the efflux assays except that the empty proteoliposomes, without loading 15 mM $MgCl_2$ and 0.5 mM ATP-Mg, were incubated in the reaction buffer containing 15 mM $MgCl_2$, with or without adding 0.5 mM ATP-Mg.

2.6. Statistical analysis

All data were analyzed by Student's *t* test. Statistical results were presented as means ± S.D. Asterisks indicate critical levels of significance ($^{*}P < 0.05$, $^{**}P < 0.01$, and $^{***}P < 0.001$).

3. Results

3.1. Identification of Mme1 as an antagonizer of mitochondrial Mg^{2+} importers Mrs2 and Lpe10

The *mrs2Δ* mutant loses the ability to respire [10]. To identify other genes involved in mitochondrial Mg^{2+} homeostasis, we previously initiated a genetic screening to search for genes whose mutations are able to suppress the growth defect of *mrs2Δ* on non-fermentable media (Fig. 1A). *YMR166C* (hereafter called *MME1*) was isolated in this process. Deletion of *MME1* is able to reverse the growth and group II RNA splicing defects in the *mrs2Δ* mutant [17].

MME1 is a nuclear gene that encodes a protein product consisting of 368 amino acids. It is predicted to be a mitochondrial inner membrane transporter belonging to the mitochondrial carrier family [24,25]. However, little is known about the molecular function of this protein. As a first step towards the molecular characterization of Mme1, we determined its intracellular localization by confocal microscopy. As shown in Fig. 1B, the fluorescence pattern of the GFP-tagged Mme1 well overlapped that of the RFP-tagged Cox9 (subunit VIIa of cytochrome *c* oxidase [Complex IV], the terminal member of the mitochondrial inner membrane electron transport chain). This result supports that

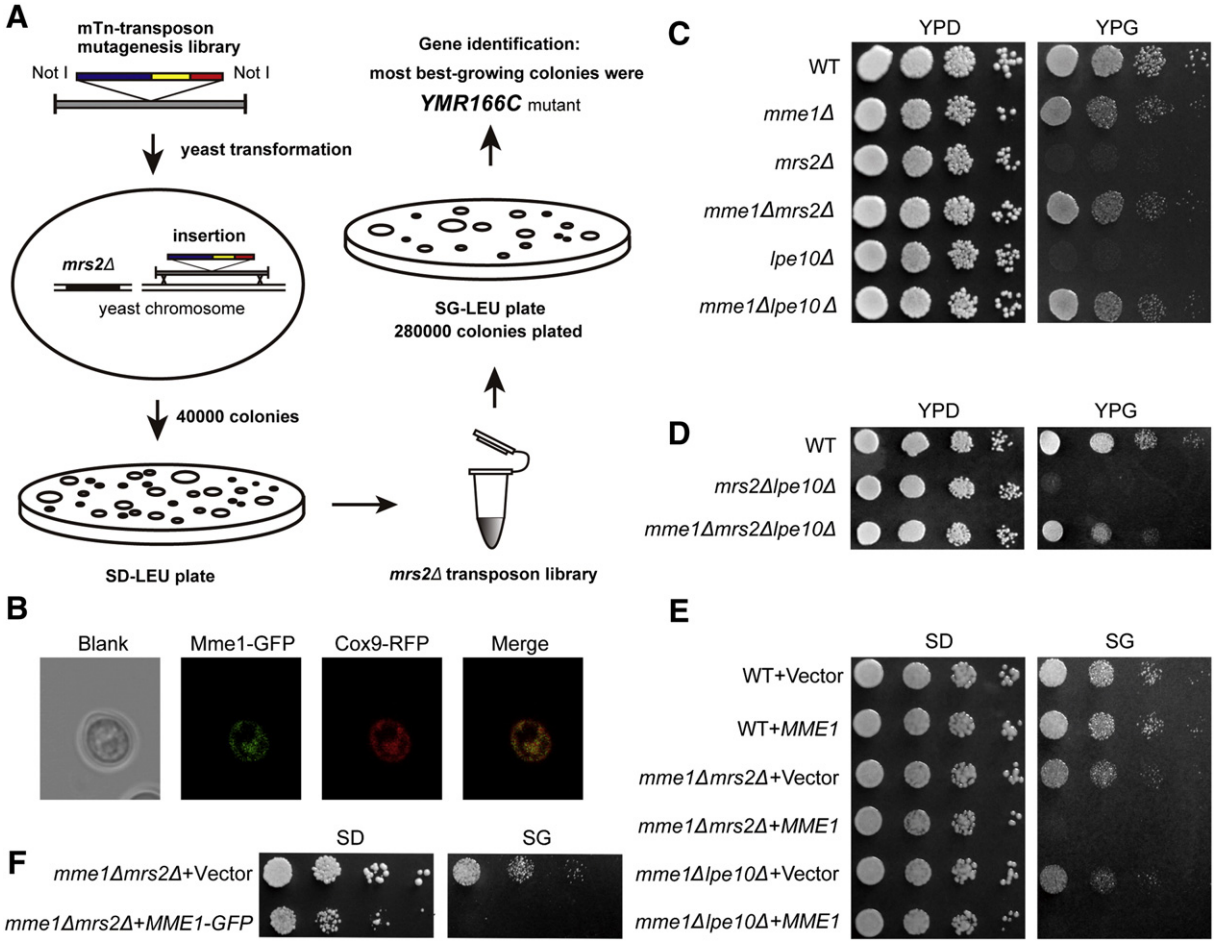

Fig. 1. Mme1 antagonizes the functions of mitochondrial Mg^{2+} importers, Mrs2 and Lpe10. (A) A schematic summarizing the genetic screening process based on mTn-lacZ/LEU2 transposon insertions to identify the suppressors of *mrs2*. (B) Subcellular localization of Mme1 in the mitochondria, as indicated by the colocalization of Mme1-GFP and Cox9-RFP. GFP and RFP were integrated into the C-terminal of the endogenous chromosomal *MME1* and *COX9*, respectively. Cox9-RFP was used to indicate the mitochondria inner membrane. (C and D) Loss of *MME1* could dramatically rescue the no-growth phenotype of *lpe10Δ* and *mrs2Δ lpe10Δ* on glycerol medium. The *mrs2Δ* here served as a positive control. (E) Additional expression of Mme1 in the double mutant of *mme1Δ lpe10Δ*, as well as *mme1Δ mrs2Δ*, could suppress the rescue. *MME1* was cloned into the single-copy centromeric expression plasmid pRS315 with *MME1*'s original promoter and terminator to ensure the endogenous expression level. (F) Expression of Mme1-GFP in the double mutant of *mme1Δ mrs2Δ* could suppress the growth on glycerol medium, suggesting that the Mme1-GFP used to determine the mitochondrial membrane localization of Mme1 is functional.

Mme1 is localized in the mitochondrial membrane, consistent with the prediction based on its primary sequence.

Although *MME1* was proposed as a candidate involved in mitochondrial Mg^{2+} metabolism, it was not known whether *mme1* suppresses the defects of *mrs2Δ* mutant by directly and independently regulating mitochondrial Mg^{2+} homeostasis. To explore how Mme1 might participate in mitochondrial Mg^{2+} homeostasis, we tested whether *mme1* could also be a suppressor of *lpe10* synchronously. We reasoned that if *MME1* deletion suppressed *mrs2Δ* by independently affecting mitochondrial Mg^{2+} homeostasis, it would also be able to suppress Mrs2's functional homologue Lpe10 as well. Spotting assay results showed that the deletion of the *MME1* gene could also completely rescue the growth defect of the *lpe10Δ* and *mrs2Δ lpe10Δ* mutant strains on non-fermentable carbon sources, as that of *mrs2Δ* (Fig. 1C and D). However, when an endogenous level of Mme1 was provided additionally in the *mme1Δ mrs2Δ* and *mme1Δ lpe10Δ* double mutants, the growth defect phenotype reappeared, proving that the growth of the double mutants was truly restored by the deletion of *MME1* (Fig. 1E). Similar results were also obtained when Mme1-GFP fusion protein was expressed in the *mme1Δ mrs2Δ* double mutant strain, suggesting that the Mme1-GFP fusion protein used for the above localization study is functional (Fig. 1F).

We speculated that *mme1* might suppress *mrs2* and *lpe10* through directly affecting mitochondrial Mg^{2+} levels. To test this hypothesis, the Mg^{2+} content in the mitochondria of *mme1Δ* was measured. As shown in Fig. 2A, disruption of *MME1* by itself led to a slight but significant increase of mitochondrial Mg^{2+} level. The *lpe10Δ* mutant carried a lower amount of Mg^{2+}, and loss of *MME1* in the *lpe10Δ* mutant resulted in a significant but not yet complete restoration of the Mg^{2+} content, similar to what was observed in the *mrs2Δ* mutant strain in both this and previous studies. This result suggests that Mme1 may function directly in the regulation of steady-state concentrations of mitochondrial Mg^{2+}. The suppression effect of *mme1* on *mrs2* and *lpe10* thus can be explained by the antagonizing effects of two factors, one enhancing and one reducing the mitochondrial Mg^{2+} level.

Because mitochondrial Mg^{2+} is critical for the splicing of group II intron RNA, which includes those of mitochondrial transcripts of *COX1* and *COB* [26], we further tested whether the deletion of *MME1* could rescue the RNA splicing defect in the *lpe10Δ* mutant, as observed in the *mrs2Δ* mutant. As shown in Fig. 2B, almost all the *COB* transcripts of the wild-type yeast were in the mature form, while there were plenty of immature pre-mRNAs of *COB* in the *mrs2Δ* and *lpe10Δ* yeast cells, consistent with previous reports from others [10,15]. Deletion of *MME1* can fully rescue the group II RNA splicing defect in the *mrs2Δ* and *lpe10Δ* disruptants, as attested by a dramatic increase of mature mRNA as well as an almost complete disappearance of immature mRNA in these double mutants (Fig. 2B).

Taken together, the deletion of *MME1* can rescue various defects observed in the *lpe10Δ* disruptant as in the *mrs2Δ* mutant, likely through an independent and opposite effect on mitochondrial Mg^{2+} homeostasis. Since Mme1 is a mitochondrial carrier protein [24], we proposed that Mme1 might act as an Mg^{2+} exporter.

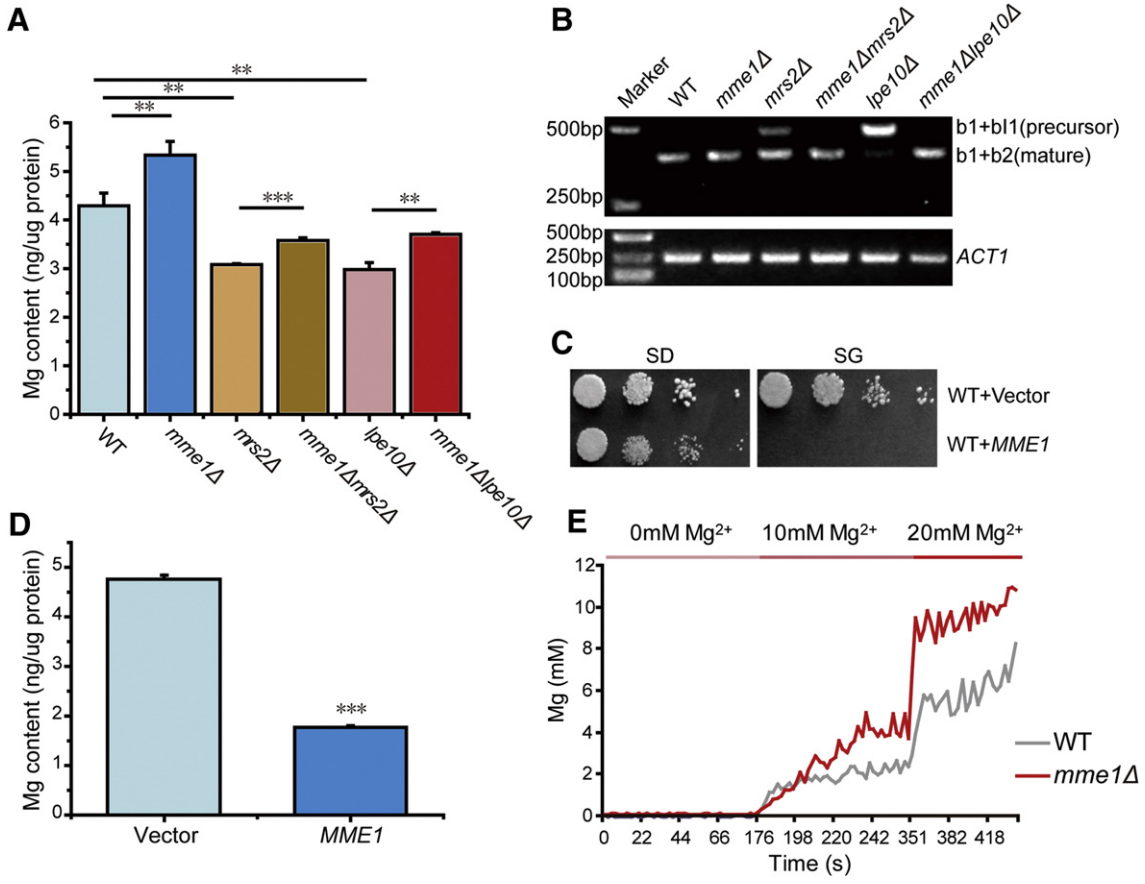

Fig. 2. Mme1 functions as a mitochondrial Mg^{2+} regulator in yeast. (A) Deletion of *MME1* could significantly restore Mg^{2+} deficiency in the mitochondria of *lpe10Δ* and *mrs2Δ* mutants. Mg^{2+} contents in the isolated mitochondria were normalized by total mitochondrial protein contents. Values are presented as mean ± S.D.; $n \geq 3$. (B) Absence of *MME1* restored group II RNA splicing defects of *mrs2Δ* and *lpe10Δ* mutants. RT-PCR assays were performed with a mixture of three oligonucleotide primers matching two different exons and one intron of *COB*. PCR product of *ACT1* was used as the loading control. (C) Overexpression of *MME1* resulted in growth deficiency on non-fermentable media with glycerol as the sole carbon source. *MME1* was cloned into a GPD promoter-driven vector, pGPD-413. (D) Overexpression of *MME1* led to a dramatic decrease of the mitochondrial Mg^{2+} content. Values are presented as mean ± S.D.; $n \geq 3$. (E) Response of mitochondrial Mg^{2+} levels to external Mg^{2+}. The change of Mg^{2+} was indicated by the use of a Mg^{2+}-sensitive fluorescence probe, mag-fura-2. The extramitochondrial Mg^{2+} concentration was stepwise raised to a final concentration of 10 mM and then to 20 mM.

3.2. Mme1 overexpression leads to mitochondrial Mg^{2+} reduction

If Mme1 mediates Mg^{2+} efflux from the mitochondria while Mrs2 and Lpe10 are responsible for Mg^{2+} influx, the phenotype of overproducing Mme1 would be quite similar to that of mutants lacking Mrs2 or Lpe10. As predicted, yeast strain overexpressing Mme1 showed a severe growth defect on glycerol medium similar to that of the *mrs2Δ* or *lpe10Δ* mutants (Figs. 1C and 2C).

Next, we sought to clarify whether the growth defect of the Mme1-overexpressing strain resulted from a decrease of mitochondrial Mg^{2+} as seen with *mrs2Δ* or *lpe10Δ* mutants. For that, the mitochondrial Mg^{2+} contents in both yeast strains transformed with an empty vector and *MME1* respectively were measured. Consistently, mitochondria of the strain overexpressing Mme1 contained a significantly lower Mg^{2+} concentration than that of the control strain (Fig. 2D).

We then sought to measure the time-course response of Mme1 to extra-mitochondrial Mg^{2+}, using an Mg^{2+}-sensitive fluorescent dye, mag-fura-2. Mitochondria were isolated from cells of wild-type and *MME1*-deleted yeast strains and transferred into a nominally Mg^{2+}-free solution to facilitate the loading of the membrane-permeant acetoxymethyl ester (AM) of mag-fura-2, activation of the probe, and determination of the basal intra-mitochondrial free Mg^{2+}. When the extra-mitochondrial Mg^{2+} concentration was increased stepwise to 10 and then to 20 mM, the fluorescent intensity ratio of 340/380 nm (340 and 380 nm are standard excitation wavelengths for the ion-bound and the free mag-fura-2, respectively) also immediately increased, indicating that Mg^{2+} transiently and instantly crossed the mitochondrial membrane. The increased rate of Mg^{2+} loading in the wild-type yeast is much lower than that of the *mme1Δ* mutant (Fig. 2E). We explain this by the fact that when Mme1 was functional, some Mg^{2+} efflux occurred, resulting in a reduced mitochondrial Mg^{2+} accumulation. All these data suggest that Mme1 works opposite to Mrs2 and Lpe10, and provide further evidence supporting the notion that Mme1 may be responsible for the efflux of mitochondrial Mg^{2+}.

3.3. Heterologous expression of yeast Mme1 in E. coli reduces its Mg^{2+} level

Mitochondria are thought to originate from proteobacteria that were taken up by a type of nucleated cell and in some aspects mimic bacterial cells such as *E. coli*. To obtain more direct and convincing evidence, the Mg^{2+} transport activity of Mme1 was examined in a heterologous biosystem in which Mme1 was expressed in *E. coli*.

As a membrane protein, Mme1 is difficult to significantly express and purify *in vitro*. Initially, little expression of Mme1 was detected in *E. coli* when a number of vectors (pET-21b, pET-28a, pGEX4T-1, pQE-80 L, and pTWIN-1) were used. Nonetheless, expression of Mme1 was finally achieved by using the pEXS-DH plasmid vector with an N-terminal HIS-tag and *E. coli* host strain *CD41 (DE3)* (*F^- ompT gal dcm lon hsdS_B(r_B^- m_B^-)* λ(DE3 [*lacI lacUV5-T7 gene 1 ind1 sam7 nin5*]) (Fig. 3A).

Results of confocal microscopy showed that the heterogeneously expressed Mme1 protein in *E. coli* localizes in the peripheral area (plasma membrane) of *E. coli*, coinciding with the presumed localization of Mme1 in the mitochondrial membrane in yeast (Fig. 3B).

We next asked whether Mme1 expression in such a foreign system could facilitate cellular Mg^{2+} efflux. Interestingly, Mme1 expression mildly but noticeably conferred *E. coli* resistance to Mg^{2+} stress, but not to Zn^{2+} or Na^+ (Fig. 3C). The growth differences were further confirmed by culturing the vector control and Mme1-expressing *E. coli* strains in corresponding liquid media. When cultured in LB medium supplemented with only IPTG or together with 2 mM Zn^{2+} and 200 mM Na^+, there were no significant differences between the vector control and the Mme1-expressing *E. coli* strain. However, the Mme1-expressing *E. coli* strain showed significant growth advantages over the vector control in LB medium with 200 mM Mg^{2+}, indicating that Mme1 expression specifically confers Mg^{2+} resistance (Fig. 3D).

Further analysis of cellular Mg^{2+} contents indicated that expression of Mme1 indeed significantly reduced the Mg^{2+} level of the cells (Fig. 3E). The reduction of Mg^{2+} contents here is not as dramatic as in Fig. 2D, likely because of the foreign or non-native nature of Mme1 when expressed in *E. coli*. Nonetheless, a decreased Mg^{2+} concentration enables the Mme1-expressing *E. coli* to be resistant to Mg^{2+} excess. These results suggest that Mme1 is necessary and sufficient in mediating mitochondrial Mg^{2+} efflux.

3.4. The purified Mme1 can mediate Mg^{2+} export in vitro when reconstituted into liposomes

The above data together strongly suggest that Mme1 is an Mg^{2+} exporter. Despite this, direct evidence of Mme1 as an Mg^{2+} exporter is still lacking. One definite evidence would be a transport measurement experiment using purified Mme1 protein performed in a clean *in vitro* system—proteoliposomes.

To obtain purified Mme1, we screened for detergents that might be able to dissolve it. Mme1 was solubilized most efficiently in 2% Fos-choline-12 (FC12), better than DDM, while other detergents, including 2% CHAPS, were not very effective on Mme1 (Table 1). Mme1 is purified by Ni-NTA agarose column and Sephadex 200 column sequentially from total proteins (Fig. 3A) (more details in Materials and methods section).

Purified Mme1 was then reconstituted into yeast total-lipid-based liposomes as described in the Materials and methods section. TMHMM analysis suggests that Mme1 possesses two transmembrane domains within the 115–168 amino acid residues region. To analyze the orientation of the reconstituted Mme1 in the proteoliposomes, they were treated separately with two proteases—trypsin and chymotrypsin. Pure recombinant Mme1 was also subjected to the same treatments to work as controls. Protease digestion of the pure Mme1 and proteoliposome-incorporated Mme1 led to an almost complete disappearance of the protein band in SDS-PAGE (Fig. 4A). This result indicates that Mme1 was preferentially inserted into proteoliposomes with most of it exposed to the exterior of the liposomes in our reconstituted samples. Were the orientation opposite, little or only part of the amino acids between the two predicted transmembrane domains of Mme1 would have been digested. Worth noting is that this predicted orientation of Mme1 in the membrane is opposite to that of AtMrs2-10, which was preferentially inserted into proteoliposomes with most of it exposed to the interior of the liposomes [22]. This difference is consistent with their opposite functions in Mg^{2+} transport with AtMrs2-10 as Mg^{2+} importer whereas Mme1 as a candidate of Mg^{2+} exporter.

According to this topology model, we predicted that after protease digestion, a 6 KD polypeptide of Mme1 imbedded within the liposomes would be protected and undigested. However, we failed to detect this predicted 6 KD polypeptide band in our SDS-PAGE gel. One possible explanation for the failure might be the small size and high hydrophobicity of this protein portion. Therefore, at this moment, the proposed model remains only a favorite possibility (Fig. 4B).

The Mg^{2+} export activity of Mme1 was subsequently measured. To ensure more complete Mg^{2+} transport, the Mme1 proteoliposomes packed with Mg^{2+} buffer were incubated with Mg^{2+}-free reaction buffer at 30 °C for 2 h. After the reaction, the contents of the remaining Mg^{2+} within the proteoliposomes was determined by ICP-MS. The more Mg^{2+} remaining in the proteoliposomes, the less Mg^{2+} was transported out. As shown in Fig. 4C, a significant decrease in the internal Mg^{2+} content was observed when liposomes were incorporated with Mme1, indicating that the reconstituted Mme1 was able to mediate Mg^{2+} efflux out of liposomes in the presence of an outward-directed Mg^{2+} gradient. Liposome integrity was intact as the K^+ packed within the liposomes did not change appreciably (Fig. 4D). Interestingly, we observed that the Mg^{2+} export reaction occurred only in the presence of ATP-Mg packed in the proteoliposomes. In the absence of ATP,

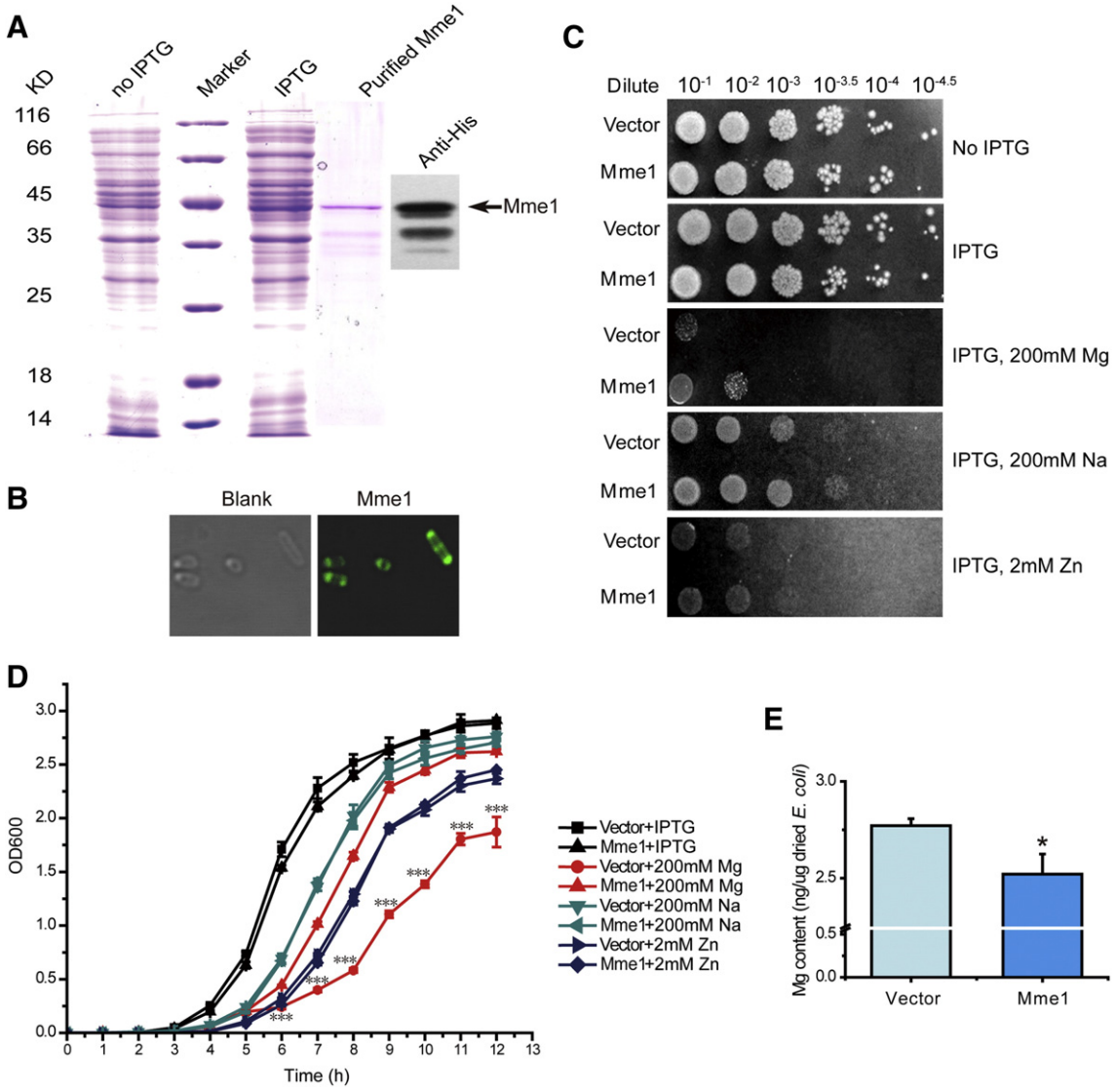

Fig. 3. Mme1 regulates Mg^{2+} homeostasis when heterologously expressed in *E. coli*. (A) Coomassie brilliant blue staining result of protein samples from *MME1*-transformed *E. coli* cells with or without induction by IPTG, and purified Mme1, and purified Mme1 blotted by antibody against His tag in the N-terminal of Mme1 protein. At least some of the impurities in the purified Mme1 were due to partially degraded Mme1 as shown by Western blotting results. (B) Plasma membrane-localization of Mme1 in *E. coli*. Immunofluorescence assays were carried out in *E. coli* CD41 (DE3) cells transfected with a HIS-tagged Mme1. (C) Mme1-expressing *E. coli* cells were mildly, but selectively, resistant to Mg^{2+} when stressed by various metal ions. Spotting assays of *E. coli* cells were performed on LB medium supplemented with or without IPTG, together with 200 mM Mg^{2+}, 2 mM Zn^{2+}, and 200 mM Na^{+} respectively. A total of 200 mM Na^{+} served as an osmolarity control to exclude the possibility that Mme1-expressing *E. coli* cells were resistant to the higher osmolarity caused by 200 mM Mg^{2+} instead of to Mg^{2+} per se. (D) The growth of *E. coli* strains transformed with vector or Mme1 were confirmed in corresponding liquid medium. (E) Expression of Mme1 in *E. coli* decreased Mg^{2+} concentration within the cells. The contents of Mg^{2+} in *E. coli* cells were measured by ICP-MS and normalized by the gross dry weight of *E. coli* cells. Values are presented as mean ± S.D.; $n \geq 3$.

the exporting activity almost disappeared (Fig. 4E). Therefore, it seems that ATP is indispensable for the transport of Mg^{2+} by Mme1.

We further explored the role of ATP in this process—primarily concerning whether the hydrolysis of ATP is necessary for the transport of Mg^{2+}. To address this question, ATPγS, a common ATP analog, which cannot be hydrolyzed, was used to replace ATP to test whether ATPγS can also mediate the transport. In the presence of ATPγS or in the absence of ATP hydrolysis, an obvious reduction, albeit less dramatic than ATP, of Mg^{2+} within proteoliposomes was also observed (Fig. 4F). This result suggests that ATP-Mg may act as a substrate for the transportation independent of ATP hydrolysis. As some structural differences between ATP and ATPγS exist, Mme1 may prefer the native ATP to non-native ATPγS in facilitating Mg^{2+} transport.

We also measured the importing activity of Mg^{2+} by Mme1 *in vitro*. The importation assay was similar to the exportation assay except that the Mg^{2+} and ATP were added to the reaction buffer instead of within the liposomes. When Mme1 was reconstituted into the liposomes, the Mme1 could also transport some Mg^{2+} into the liposomes in an ATP-dependent manner (Fig. 4G). However, the influx activity is much less robust than the efflux activity. These results suggest that Mme1 has a preference for exporting over importing Mg^{2+}.

Table 1
Detergents screening for Mme1 solubilization.

Detergent	% Added	Solubilization efficiency
3-[(3-Cholamidopropyl)dimethylammonio]-propanesulfonic acid (CHAPS)	1–2	−
Sodium cholate	1–2	−
Lauryldimethyl amine oxide (LDAO)	1–2	−
n-Dodecyl-β-D-maltoside (DDM)	1–2	+
Fos-choline-12 (FC12)	1–2	++

++, high solubilization; +, low solubilization; −, little solubilization.

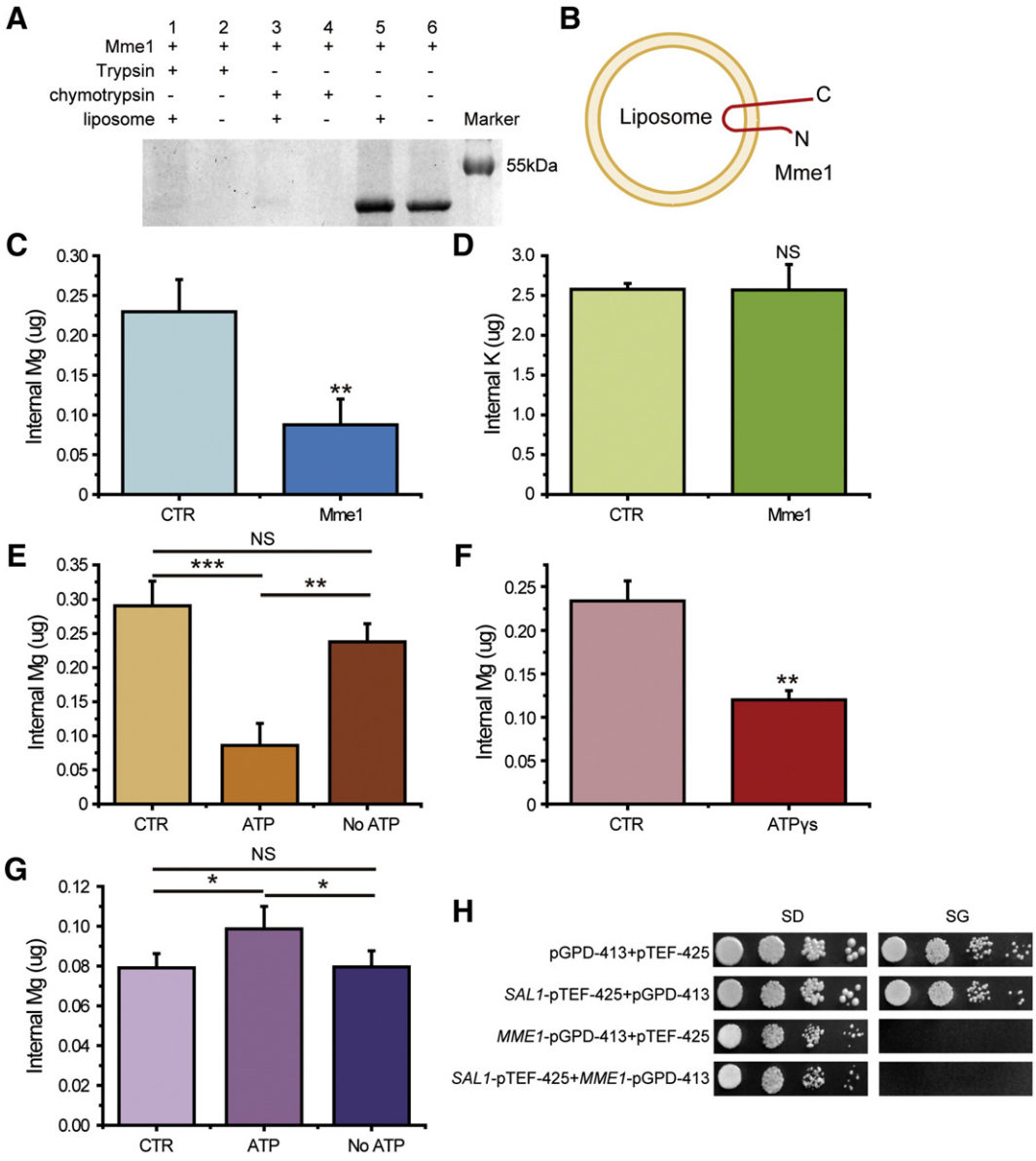

Fig. 4. Mg^{2+} efflux mediated by Mme1 in proteoliposomes *in vitro*. (A) Determination of the Mme1 orientation in proteoliposomes with protease protection assays. Protease/Mme1 ratio was 1: 50. After incubation at 30 °C for 30 min, protease digestion was terminated by the addition of SDS-PAGE sample buffer and heated for 10 min at 98 °C. The peptide that would be protected from the digestion (the two transmembrane domains plus the region in between) is smaller than 6KD (amino acid 115–168 region) and it might be too small and hard to detect here under this condition. (B) A likely representation of the topology of Mme1 in proteoliposomes. "N" and "C" stand for the N- and C-terminals of Mme1, respectively. (C) Mg^{2+} efflux mediated by Mme1-reconstituted liposomes with 0.5 mM ATP-Mg. The internal Mg^{2+} remaining in the liposomes after reactions was determined. (D) K^{+} contents within liposomes incorporated with or without Mme1. (E) Mg^{2+} transporting activities of Mme1-incorporated liposomes in the absence of ATP-Mg. (F) Mg^{2+} efflux activities of Mme1-incorporated liposomes with 0.5 mM non-hydrolysable ATP analogue ATP-γ-S. (G) Mg^{2+} influx activities of Mme1-incorporated liposomes. Values in C, D, E, F, and G are presented as mean ± S.D.; $n \geq 3$. NS stands for no significance. (H) Overexpression of *SAL1*, which exchanges ATP-Mg into and Pi out of mitochondria, cannot rescue the growth defect of *MME1* overexpression on respiration media.

There are some other mitochondrial carrier proteins utilizing ATP-Mg as the exchanger for Pi. However, the functions of these carrier proteins are to transport adenine nucleotides across the mitochondrial inner membrane, and thus regulate the homeostasis of ATP but not Mg^{2+} within mitochondria as other ATP/ADP carriers. In yeast, Sal1 is the only ATP-Mg/Pi carrier discovered so far which transports ATP-Mg into the mitochondrial matrix and Pi out of the mitochondrial matrix [27–29]. Therefore, we wondered whether or not Sal1 functions by transporting Mg^{2+} into mitochondria, thereby working opposite to Mme1. While overexpressing Sal1 in the Mme1-overexpressing yeast strain, we found that Sal1 did not suppress the phenotype of Mme1 overexpression, indicating that Sal1 and Mme1 may not have functional interaction (Fig. 4H). The reason why overexpression of Sal1, an ATP-Mg importer, cannot rescue the phenotype of overexpression of Mme1 may be that the accessory Mg^{2+} entering with ATP are physiologically too minor to appreciably alter the mitochondrial Mg^{2+} level.

The proteoliposome experiment provided direct evidence in supporting the hypothesis that yeast Mme1 mediates Mg^{2+} transport, mainly the efflux of Mg^{2+}. In addition, accessory proteins are not required for Mme1's function, or in other words, Mme1 is necessary and sufficient for Mg^{2+} export.

3.5. Mitochondria can supplement Mg^{2+} to cytoplasm for growth in Mg^{2+}-depleted condition

Following the molecular characterization of Mme1 both *in vivo* and *in vitro* as described above, we then analyzed the physiological function of Mg^{2+} efflux from mitochondria mediated by Mme1. Our primary

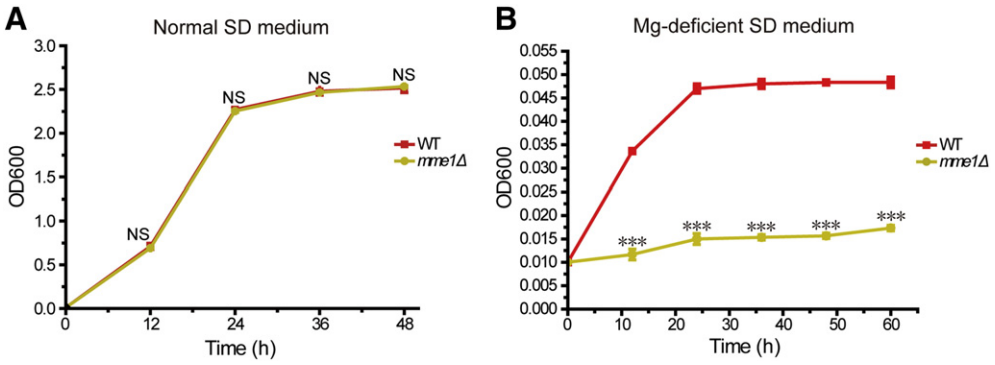

Fig. 5. *MME1* provides a growth advantage under Mg^{2+}-deficient conditions. (A) Wild-type and *mme1Δ* mutant yeast strains displayed similar growth rates in normal growth conditions. Yeast was cultured in normal SD media at 30 °C and OD_{600} measurements were carried out every 12 h. The original inoculation OD_{600} was 0.01. (B) The growth of *mme1Δ* mutant yeast strain was hindered when transferred from normal medium to Mg^{2+}-deficient medium. The growth curves of these yeast strains in SD-Mg^{2+} media (synthetic media without Mg^{2+}) were determined as described in A. Values in A and B are presented as mean ± S.D.; $n \geq 3$. NS stands for no significance.

investigation concerned whether Mme1 contributes to the cytoplasmic Mg^{2+} levels when external Mg^{2+} is lacking. To address this concern, the growth rates of the wild-type and the *mme1Δ* mutant yeast strains were monitored. As shown in Fig. 5A, these two yeast strains exhibited identical growth rates under normal growth conditions. However, the *mme1Δ* mutant grew much worse than the wild-type control when they were transferred from normal medium to Mg^{2+}-deficient medium (Fig. 5B). This can be explained by the failure of Mg^{2+} release from the *mme1Δ* mitochondria when the cytosol is in dire need of Mg^{2+}. These data support that mitochondria are helpful Mg^{2+} pools when the cell is stressed by an acute Mg^{2+} shortage. In Mg^{2+}-deficient growth conditions, the Mme1-mediated release of Mg^{2+} from mitochondria into the cytosol might be important for the cell although this might compromise the mitochondria's own functions.

4. Discussion

Mme1 has been identified as the first yeast mitochondrial Mg^{2+} exporter by a genome-wide screening. Besides suppressing the growth defect in *mrs2Δ* and *lpe10Δ* mutants, deletion of *MME1* can also rescue group II RNA splicing defects and restore the decreased mitochondrial Mg^{2+} content in these two mutant strains. Further studies revealed that Mme1 can regulate the mitochondrial Mg^{2+} efflux in yeast, mediate the Mg^{2+} transport out of the cells when heterologously expressed in *E. coli*, and display Mg^{2+} output activities when purified Mme1 is inserted into liposomes *in vitro*, providing definite evidence that Mme1 is a yeast mitochondrial Mg^{2+} exporter.

4.1. Mme1 as a mitochondrial Mg^{2+} exporter

There are only two Mg^{2+} transport proteins that have been previously purified and reconstituted into liposomes—*T. maritima* CorA and *Arabidopsis* AtMrs2-10 [22,30]. In this work, through the use of proteoliposome, we provide compelling evidence showing Mme1 as a mitochondrial Mg^{2+} exporter.

In the proteoliposome experiments, we found that the transport of Mg^{2+} by Mme1 is dependent on ATP, although the hydrolysis of ATP is not required. We suspected that ATP may be transported together with Mg^{2+}. To address this possibility, we measured the efflux of ATP from ATP-Mg loaded liposomes reconstituted with Mme1. However, there is no obvious efflux of ATP out of the liposomes. Because the amount of ATP loaded into the liposomes is only 1/30th of that of Mg^{2+}, if the ATP is transported together with Mg^{2+} at a ratio of 1:1, we predict that only a maximum of 1/30th of the initial Mg^{2+} could be transported out. However, as shown in our results (Fig. 4C and E), ~50% of the total Mg^{2+} was transported out from the liposomes. Therefore, we suspect that the transport is mediated by an ATP/ATP-Mg exchange. This speculated transportation mechanism requires further experimental studies to prove.

Our *in vitro* studies suggest that Mme1 preferentially exports Mg^{2+}, though it also carries much less robust Mg^{2+} importing activity. However, the *in vivo* results indicate that Mme1 only functions as an Mg^{2+} exporter. One possible explanation for this is that in the context of *in vivo* conditions, the net result of these transporting activities might only present as Mg^{2+} export. Therefore, it may also be the same with Mrs2. However, only the importing activity of the AtMrs2 has been measured while the exporting activity of it has not yet been measured successfully so far [22]. Another possible explanation is that *in vivo* there might be other accessory proteins interacting with Mme1, acting as molecular switches to control the orientation of Mg^{2+} transportation. Some other ion transporters indeed have been shown to function in this manner. For example, the central α(1) pore-forming subunit (Ca(V)α(1)) interacts with different accessory subunits to control the current of calcium [31]. In the case of Mrs2, Mrs2 proteins form heteromultimers with Lpe10 and work together with Lpe10 to mediate the import of Mg^{2+} into mitochondria [16]. It is possible that the interactions between Mrs2 and Lpe10 might control the orientation of Mg^{2+} transport. Alternatively, there may also be other accessory proteins to help control this process.

4.2. Regulatory effects of Mme1 on Mg^{2+} homeostasis in mitochondria and cytosol

Decrease of mitochondrial Mg^{2+} in *the mrs2Δ*, *lpe10Δ* mutants or *MME1*-overexpressing strains causes growth defect on glycerol media, as a result of severe disruption of respiration because several critical enzymatic reactions in the electron transport chain require Mg^{2+} [10,11]. Additional functions modulated by Mg^{2+} within mitochondria are anion channels, H^+ gradients, and membrane potentials across the mitochondrial membrane [1]. In other words, mitochondrial Mg^{2+} is involved in many processes and it is critical to maintain its proper concentration in a tight range because even a tiny alteration may affect the functions of mitochondria and even the fate of the whole cell.

As the first mitochondrial Mg^{2+} exporter identified, the role of Mme1 on the overall control of mitochondrial Mg^{2+} must be considered in the context of the whole cell. On the one hand, perturbation of *MME1* expression corresponds to mitochondrial Mg^{2+} changes; on the other hand, isolated normal mitochondria with intact *MME1* or intact mitochondrial Mg^{2+} homeostasis systems are still sensitive to the external Mg^{2+} variation, shown by the fact that the internal Mg^{2+} concentrations fluctuate with the added Mg^{2+} levels. Therefore, mitochondrial Mg^{2+} homeostasis is likely subjected to multiple levels of control even in a unicellular eukaryotic organism. The plasma membrane–resident importers may control the amount of Mg^{2+} imported, while organelles such as the vacuole provide additional

buffers for cytosolic Mg^{2+} maintenance. On top of these controls, which already provide a relatively constant Mg^{2+} environment for the mitochondria, the importers and exporters in the mitochondria themselves then work together intricately to fine-tune the mitochondrial Mg^{2+} level. Expression perturbation of either of these partners by overexpression or removal may shift the Mg^{2+} balance. In our opinion, the exporting role of Mme1 likely acts as a second checkpoint to maintain an accurate balance of Mg^{2+}` concentration within mitochondria under normal growth conditions.

On the other hand, under Mg^{2+}-deficient states, mitochondria can additionally supply some precious Mg^{2+} to the cytosol. Previous studies in mammalian cells have already uncovered a necessity of the maintenance of proper Mg^{2+} levels for the cell cycle, cell proliferation, and cell differentiation, all of which would be greatly inhibited when cellular available Mg^{2+} is limited or reduced [1]. As shown by our results in yeast, the *mme1Δ* mutants can hardly grow in Mg^{2+}-depleted fermentable medium, suggesting the significance of the contribution from the mitochondrion when external Mg^{2+} is limited. In the context of a tightly controlled mitochondrial Mg^{2+} homeostasis, we suspect that the contribution of mitochondria to cytosolic Mg^{2+} may not be too dramatic. As shown in Figs. 1C and 2A, with only a decrease of ~30% in mitochondrial Mg^{2+} content, the *mrs2Δ and lpe10Δ* mutants are unable to grow on glycerol medium. It can be inferred that the mitochondria must maintain a narrow range of Mg^{2+} concentrations themselves, and therefore cannot usually release too much Mg^{2+} into the cytosol without sacrificing their own functions.

Author Contributions

Conceived and designed the experiments: YC, SZ, FS, and BZ. Performed the experiments: YC, SZ, JW, XW, BG, and QF. Analyzed the data: YC and SZ. Wrote the paper: YC, SZ, and BZ.

Conflict of interest

The authors declare no conflict of interest.

Acknowledgments

We greatly appreciate the generous advices on proteoliposome experiments from Dr. Qiang Zhou (Tsinghua University, Beijing, China). We thank Richard Jiang Yang (Dartmouth College, New Hampshire, USA) for language editing. This work was supported by grants from the National Science Foundation of China (31123004, 31301020). One of the authors, Yixian Cui, was supported in part by the Postdoctoral Fellowship of Center for Life Sciences.

References

[1] A.M. Romani, Cellular magnesium homeostasis, Arch. Biochem. Biophys. 512 (2011) 1–23.
[2] A. Hartwig, Role of magnesium in genomic stability, Mutat. Res. 475 (2001) 113–121.
[3] C.G. Musso, Magnesium metabolism in health and disease, Int. Urol. Nephrol. 41 (2009) 357–362.
[4] C.W. Helmut Geiger, Magnesium in disease, Clin Kidney J 5 (2012) i25–i38.
[5] M. Horlitz, P. Klaff, Gene-specific trans-regulatory functions of magnesium for chloroplast mRNA stability in higher plants, J. Biol. Chem. 275 (2000) 35638–35645.
[6] C.W. MacDiarmid, R.C. Gardner, Overexpression of the *Saccharomyces cerevisiae* magnesium transport system confers resistance to aluminum ion, J. Biol. Chem. 273 (1998) 1727–1732.
[7] A. Graschopf, J.A. Stadler, M.K. Hoellerer, S. Eder, M. Sieghardt, S.D. Kohlwein, R.J. Schweyen, The yeast plasma membrane protein Alr1 controls Mg2+ homeostasis and is subject to Mg2 + -dependent control of its synthesis and degradation, J. Biol. Chem. 276 (2001) 16216–16222.
[8] G. Borrelly, J.C. Boyer, B. Touraine, W. Szponarski, M. Rambier, R. Gibrat, The yeast mutant vps5Delta affected in the recycling of Golgi membrane proteins displays an enhanced vacuolar Mg2+/H+ exchange activity, Proc. Natl. Acad. Sci. U. S. A. 98 (2001) 9660–9665.
[9] N.P. Pisat, A. Pandey, C.W. Macdiarmid, MNR2 regulates intracellular magnesium storage in *Saccharomyces cerevisiae*, Genetics 183 (2009) 873–884.
[10] G. Wiesenberger, M. Waldherr, R.J. Schweyen, The nuclear gene MRS2 is essential for the excision of group II introns from yeast mitochondrial transcripts in vivo, J. Biol. Chem. 267 (1992) 6963–6969.
[11] J. Gregan, M. Kolisek, R.J. Schweyen, Mitochondrial Mg(2+) homeostasis is critical for group II intron splicing in vivo, Genes Dev. 15 (2001) 2229–2237.
[12] M. Kolisek, G. Zsurka, J. Samaj, J. Weghuber, R.J. Schweyen, M. Schweigel, Mrs2p is an essential component of the major electrophoretic Mg2+ influx system in mitochondria, EMBO J. 22 (2003) 1235–1244.
[13] D.M. Bui, J. Gregan, E. Jarosch, A. Ragnini, R.J. Schweyen, The bacterial magnesium transporter CorA can functionally substitute for its putative homologue Mrs2p in the yeast inner mitochondrial membrane, J. Biol. Chem. 274 (1999) 20438–20443.
[14] G. Zsurka, J. Gregan, R.J. Schweyen, The human mitochondrial Mrs2 protein functionally substitutes for its yeast homologue, a candidate magnesium transporter, Genomics 72 (2001) 158–168.
[15] J. Gregan, D.M. Bui, R. Pillich, M. Fink, G. Zsurka, R.J. Schweyen, The mitochondrial inner membrane protein Lpe10p, a homologue of Mrs2p, is essential for magnesium homeostasis and group II intron splicing in yeast, Mol. Gen. Genet. 264 (2001) 773–781.
[16] G. Sponder, S. Svidova, R. Schindl, S. Wieser, R.J. Schweyen, C. Romanin, E.M. Froschauer, J. Weghuber, Lpe10p modulates the activity of the Mrs2p-based yeast mitochondrial Mg2+ channel, FEBS J. 277 (2010) 3514–3525.
[17] J. Wang, Q.W. Fan, B. Zhou, A transposon-based genetic screen in *Saccharomyces cerevisiae* reveals a role of YMR166C in mitochondrial magnesium homeostasis, Prog. Biochem. Biophys. 37 (2010) 36–41.
[18] R.D. Gietz, R.H. Schiestl, Applications of high efficiency lithium acetate transformation of intact yeast cells using single-stranded nucleic acids as carrier, Yeast 7 (1991) 253–263.
[19] D. Mumberg, R. Muller, M. Funk, Yeast vectors for the controlled expression of heterologous proteins in different genetic backgrounds, Gene 156 (1995) 119–122.
[20] Y. Cui, S. Zhao, Z. Wu, P. Dai, B. Zhou, Mitochondrial release of the NADH dehydrogenase Ndi1 induces apoptosis in yeast, Mol. Biol. Cell 23 (2012) 4373–4382.
[21] G. Grynkiewicz, M. Poenie, R.Y. Tsien, A new generation of Ca2+ indicators with greatly improved fluorescence properties, J. Biol. Chem. 260 (1985) 3440–3450.
[22] S. Ishijima, Z. Shigemi, H. Adachi, N. Makinouchi, I. Sagami, Functional reconstitution and characterization of the Arabidopsis Mg(2+) transporter AtMRS2-10 in proteoliposomes, Biochim. Biophys. Acta 1818 (2012) 2202–2208.
[23] E.R. Geertsma, N.A. Nik Mahmood, G.K. Schuurman-Wolters, B. Poolman, Membrane reconstitution of ABC transporters and assays of translocator function, Nat. Protoc. 3 (2008) 256–266.
[24] R. Belenkiy, A. Haefele, M.B. Eisen, H. Wohlrab, The yeast mitochondrial transport proteins: new sequences and consensus residues, lack of direct relation between consensus residues and transmembrane helices, expression patterns of the transport protein genes, and protein-protein interactions with other proteins, Biochim. Biophys. Acta 1467 (2000) 207–218.
[25] F. Palmieri, Mitochondrial transporters of the SLC25 family and associated diseases: a review, J. Inherit. Metab. Dis. 37 (2014) 565–575.
[26] F. Michel, J.L. Ferat, Structure and activities of group II introns, Annu. Rev. Biochem. 64 (1995) 435–461.
[27] X.J. Chen, Sal1p, a calcium-dependent carrier protein that suppresses an essential cellular function associated With the Aac2 isoform of ADP/ATP translocase in Saccharomyces cerevisiae, Genetics 167 (2004) 607–617.
[28] J. Traba, E.M. Froschauer, G. Wiesenberger, J. Satrustegui, A. Del Arco, Yeast mitochondria import ATP through the calcium-dependent ATP-Mg/Pi carrier Sal1p, and are ATP consumers during aerobic growth in glucose, Mol. Microbiol. 69 (2008) 570–585.
[29] J. Laco, I. Zeman, V. Pevala, P. Polcic, J. Kolarov, Adenine nucleotide transport via Sal1 carrier compensates for the essential function of the mitochondrial ADP/ATP carrier, FEMS Yeast Res. 10 (2010) 290–296.
[30] J. Payandeh, C. Li, M. Ramjeesingh, E. Poduch, C.E. Bear, E.F. Pai, Probing structure-function relationships and gating mechanisms in the CorA Mg2+ transport system, J. Biol. Chem. 283 (2008) 11721–11733.
[31] W.A. Catterall, Structure and regulation of voltage-gated Ca2+ channels, Annu. Rev. Cell Dev. Biol. 16 (2000) 521–555.